SAR Images Segmentation Using Mixture of Gamma Distribution

Ali El Zaart[1], Djemel Ziou[1], Shengrui Wang[1], Qingshan Jiang[1], Goze Bertin Bénié[2]
[1]Laboratoire de vision et traitement d'images
[2]Centre d'applications et de recherches en télédétection (CARTEL)
Université de Sherbrooke
Sherbrooke, Quebec, Canada J1K 2R1
{elzaart, ziou, wang, jiang}@dmi.usherb.ca and gbenie@courrier.usherb.ca

Abstract

This paper presents a new algorithm for SAR images segmentation based on thresholding technique. Histogram of SAR images is assumed to be a combination of Gamma distribution. The maximum-likehood technique is therefore used to estimate the histogram parameters. Thresholds are selected at the valleys of a multi-modal histogram by minimizing the discrimination error between the classes of pixels in the image. When this algorithm is tested on artificial histograms, an accurate estimate of their parameters is obtained. The algorithm is applied to several RADARSAT SAR images, with the number of looks for each image being 4 or 8. The results obtained are promising.

Keywords: SAR image segmentation, Gamma distribution, multi-modal histogram.

1 Introduction

The speckle appearing on SAR images is a natural phenomenon generated by the coherent processing of radar echoes [1, 7, 8]. The presence of speckle not only reduces the interpreter's ability to resolve fine detail, but also makes automatic segmentation of such images difficult. Generally, segmentation of a SAR image falls into two categories: 1) segmentation based on grey levels and 2) segmentation based on texture. The present paper deals with SAR images segmentation based on grey levels. We classify pixels into classes by selecting thresholds T_i at the valleys of a multi-modal histogram (see figure 1). The rule for thresholding an image $I(x,y)$ is given as:

$$R(x,y) = \begin{cases} L_1 & \text{if } I(x,y) > T_{M-1} \\ L_2 & \text{if } T_{M-2} < I(x,y) \leq T_{M-1} \\ \cdot & \\ \cdot & \\ L_M & \text{if } I(x,y) \leq T_1 \end{cases} \quad (1)$$

where M is the number of modes in the histogram. The problem of segmentation in this case is thus a problem of estimating the thresholds. Many threshold selection methods have been proposed and are summarized in [10]. Several methods use a camera image such that the distribution function is Gaussian [2, 3, 9]. In our case, we assume that the distribution function of filtered SAR images is a Gamma function. Usually, speckle distribution in amplitude SAR images can be modeled by K-distribution. If the image contains only one class, we can estimate the statistics of the histogram by using K-distribution. In ship detection for example, we are interested in only one region, so we can use K-distribution in this case [6]. But if the image has more than one class, estimation of the statistics using K-distribution is difficult. We propose a solution for this problem by using a Gamma distribution. The Gamma function in homogeneous areas is known to be [5]:

$$f(x,\mu,N) = \frac{2q}{\mu}\frac{N^N}{(N-1)!}\left(\frac{qx}{\mu}\right)^{2N-1} e^{-N\left(\frac{qx}{\mu}\right)^2} \quad (2)$$

where $q = \frac{\Gamma(N+0.5)}{\sqrt{(N)}\Gamma(N)}$, x is the intensity of the pixel, μ is the mean value of the distribution and N is the number of looks. Consequently, the SAR image histogram is a linear combination of several Gamma functions. Each mode in the histogram is a Gamma function and represents a class in this image. Thus, each class is defined by its mean μ and *a priori* probability P values (see Figure 1). In this paper, the maximum-likelihood technique is used to estimate these statistics. We assume that N and M are known. After estimating the histogram parameters, we select thresholds at the valleys of a multi-modal histogram by minimizing the error in discrimination between the classes in the image.

The paper is organized as follows, section 2 will describe the estimation of the histogram parameters. In section 3, we will present the method of estimation thresholds. Finally, in section 4, we will test the thresholding method on artificial histograms and apply it to real SAR images.

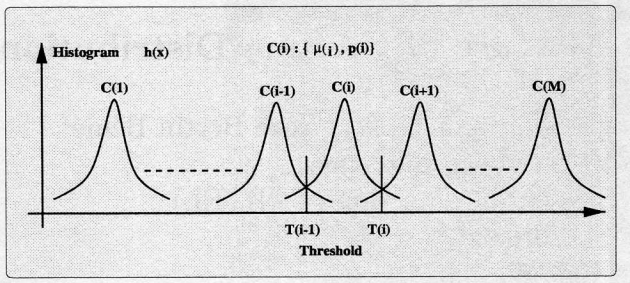

Figure 1: Multi-modal histogram.

2 Histogram Approximation

In this section, we estimate the SAR image histogram parameters based on the work of Ziou [3]. He estimated the camera image histogram parameters by using the Gaussian maximum likelihood technique. As the SAR image histogram is a linear combination of several Gamma functions, we use the Gamma maximum likelihood technique to estimate the histogram parameters (μ, P).

Let a SAR image histogram $h(x)$ have M modes (see Figure 1). It can be seen as an estimation of Gamma probability density $p(X/\Theta)$, where $X = (x_1, ..., x_H)$ is the random vector, the random variable x_i is the abscissa of the histogram, and $\Theta = (\theta_1, ..., \theta_M)$ is the parameter vector. This means that the determination of a parameter θ_i and the *a priori* probability $P(i)$ of each mode is such that $h(x_k) = p(x_k/\Theta) = \sum_{j=1}^{M} p(x_k/j, \theta_j)P(j)$. Thus, the problem of determining $\Theta = (\theta_1, ..., \theta_M)$ and $(P(1), ..., P(M))$ becomes:

$$max_{\Theta} p(X, \Theta) \tag{3}$$

with the constraints: $P(i) \geq 0 \quad \forall i \in [1, M]$ and $\sum_{i=1}^{M} P(i) = 1$. These constraints permit us to take into consideration *a priori* probabilities $P(i)$. Using Lagrange multipliers, we maximize the following function:

$$\begin{aligned} \phi(X, \Theta, \Lambda) &= ln(p(X/\Theta)) + \lambda_1(1 - \sum_{i=1}^{M} P(i)) \\ &\quad + \lambda_2 P(1) + ... + \lambda_{M+1} P(M) \end{aligned} \tag{4}$$

where Λ are the Lagrange multipliers. For convenience, we replaced the function $p(X/\Theta)$ in (eq. 3) by the function $ln(p(X/\Theta))$ in (eq. 4). The analytical resolution of this problem gives [4] :

$$\mu^2(i) = \frac{\sum_{k=1}^{H} h(x_k) p(i/x_k, \theta_i)(qx_k)^2}{\sum_{k=1}^{H} h(x_k) p(i/x_k, \theta_i)} \tag{5}$$

$$P(i) = \frac{\sum_{k=1}^{H} h(x_k) p(i/x_k, \theta_i)}{\sum_{k=1}^{H} h(x_k)} \tag{6}$$

Equations (5) and (6) allow us to calculate the parameters of each mode iteratively. This algorithm requires knowledge of the number of looks N, the number of modes M, and the initial statistics $\mu^0(i)$ and $P^0(i)$ of each mode.

3 Threshold Selection

In this section, we determine the thresholds which separate the modes in order to minimize the misclassification probability between the classes in the image. Let T_i be the threshold which separate the two classes C_i and C_{i+1} (see Figure 1). Consequently, we have $M + 1$ thresholds: $T_0, ..., T_i, ..., T_M$ where $T_0 = 0$ and $T_M =$ greatest grey level.

The misclassification probability of the class C_i for $i \in [1, M]$ is given by:

$$\begin{aligned} P_{misclass}(C_i) &= P(i)(\int_{0}^{T_{i-1}} f(x, \mu(i), N)dx \\ &\quad + \int_{T_i}^{+\infty} f(x, \mu(i), N)dx) \end{aligned} \tag{7}$$

where $f_i(x, \mu(i), N)$ is the Gamma function of the mode i and $P(i)$ is the *a priori* probability of this mode. Thus, the misclassification probability for discriminating between the classes $C_1, ..., C_i, ..., C_M$ is given by:

$$\begin{aligned} P_{misclass}(C_1, .., C_M) &= \sum_{i=1}^{M} P(i)(\int_{0}^{T_{i-1}} f(x, \mu(i), N)dx \\ &\quad + \int_{T_i}^{+\infty} f(x, \mu(i), N)dx) \end{aligned} \tag{8}$$

The question is to find $T_1, ..., T_i, ..., T_{M-1}$ which minimize the function $P_{misclass}(C_1, .., C_M)$. The solution of this problem is given by:

$$\frac{\partial}{\partial T_i} P_{misclass}(C_1, .., C_M) = 0 \tag{9}$$

We obtain the following rule:

$$P(i) f_i(T_i, \mu(i), N) = P(i+1) f_{i+1}(T_i, \mu(i+1), N) \tag{10}$$

By replacing the probability density Gamma functions f_i and f_{i+1} by their values and by taking the logarithm of each member, we find the threshold T_i for $i = 1, .., M - 1$:

$$T_i = \sqrt{\frac{Log(K_i)}{Nq^2(\frac{1}{\mu^2(i)} - \frac{1}{\mu^2(i+1)})}} \tag{11}$$

where $K_i = \frac{P(i)}{P(i+1)}(\frac{\mu(i+1)}{\mu(i)})^{2N}$

T_i is defined when $(\frac{\mu(i+1)}{\mu(i)})^{2N} > \frac{P(i+1)}{P(i)}$. There are some

special cases for which T_i is not defined. For example, consider the histograms shown in Figure 2. Each histogram in this figure is constructed from two modes. In Figure 2(a), the threshold value cannot be calculated. In Figure 2(b), the threshold can be calculated but it is incorrect. In Figure 2(c), the threshold computed is correct. On the other hand, if the number of looks is high, there is no problem for estimating thresholds. Because $(\frac{\mu(i+1)}{\mu(i)})^{2N}$ will be greater than $\frac{P(i+1)}{P(i)}$ and therefore $K_i > 1$. Otherwise, the image can be splited into sub-images and each one can be processed separately.

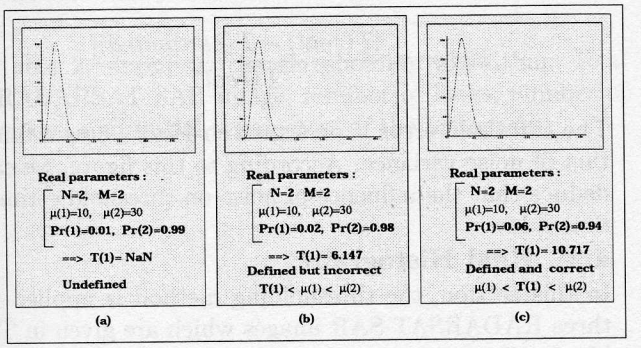

Figure 2: Different cases of threshold estimation.

4 Experimental Results

This section evaluates the thresholding method. First, the method is tested on artificial histograms. Second, it is applied to real histograms (i.e., real images). The input to the algorithm is the histogram $h(x)$, the number of looks N, the number of modes M, and the initial parameters of each mode $\mu^0(i)$ and $P^0(i)$. The output is the histogram parameters estimated by the maximum-likelihood technique using the formulas in equations (5) and (6), and the thresholds calculated using the formula in (eq. 11).

4.1 Artificial Histogram

In this section, we will test the thresholding method on ideal and noisy artificial histograms, and we will study the effect of noise on threshold estimation.

Ideal artificial histogram: Consider an ideal histogram $h(x)$. The data for this histogram are presented in Figure 2(a).

$$h(x) = \sum_{j=1}^{M} \frac{2q}{\mu(j)} \frac{N^N}{(N-1)!} (\frac{qx}{\mu(j)})^{2N-1} e^{-N(\frac{qx}{\mu(j)})^2} P(j) \quad (12)$$

We will now apply the maximum-likelihood technique to this histogram. The initial parameters are chosen as: $\mu^0(1) = 2$, $\mu^0(2) = 40, P^0(1) = 0.3$, and, $P^0(2) = 0.7$. The results are: $\mu^0(1) = 10$, $\mu^0(2) = 30$, $P^0(1) = 0.01$, and $P^0(2) = 0.99$. We can also estimate the statistics for the histograms presented in Figures 2(b) and 2(c) using the maximum-likelihood technique. However, the problem is in threshold estimation. In Figure 2(a), we can't calculate the threshold. In Figure 2(b), we have increased $P(1) = 0.02$ and decreased $P(2) = 0.98$ in order to set a defined threshold. However, this threshold is incorrect because $T(1)$ is not between $\mu(1)$ and $\mu(2)$. Next, we increase $P(1)$ and decrease $P(2)$ until we get a threshold which is both defined and correct (see Figure 2(c)). This histogram corresponds to almost the smallest possible degree of separability of two modes.

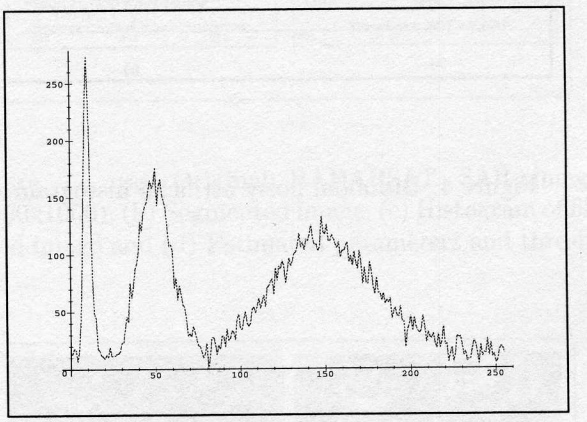

Figure 3: Noisy artificial histogram.

	Mode 1		Mode 2		Mode 3
μ_{real}	10		50		150
P_{real}	0.1		0.3		0.6
T_{real}		18.18		78.20	
$\mu_{estimed}$	10.18		50.67		156
$P_{estimated}$	0.09		0.28		0.62
$T_{estimated}$		18.98		80.23	

Table 1: Results of histogram parameter estimation

Noisy artificial histogram: Consider an ideal histogram with $M = 3$, $N_{looks} = 7$ and the real parameters presented in Table1. To this histogram is added a Gaussian white noise of variance equal to 49 (see Figure 3). We then apply the maximum-likelihood technique to this histogram. The initial parameters are chosen as: $\mu^0(1) = 30$, $\mu^0(2) = 40$, $\mu^0(3) = 200$ $P^0(1) =$

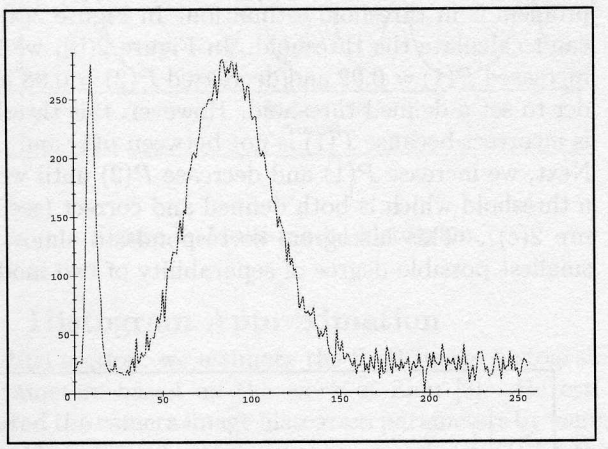

Figure 4: Bi-modal noisy artificial histogram.

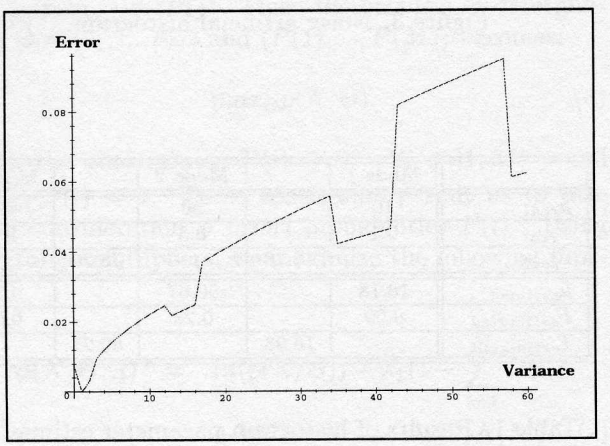

Figure 5: Error in threshold estimation as a function of noise variance.

0.7, $P^0(2) = 0.2$, and $P^0(3) = 0.1$. The results are presented in Table 1. As shown in this table, the error of the estimated parameters is low and does not greatly influence threshold estimation.

Effect of Noise on the Threshold Estimation: We will now study the effect of noise in the histogram on threshold estimation. We construct an ideal histogram with two modes $M = 2$, $N_{looks} = 4$, $\mu(1) = 10$, $\mu(2) = 90$, $P(1) = 0.1$, $P(2) = 0.9$ (see Figure 4). The threshold $T(real) = 20.30$ is calculated by using the real parameters of this histogram. To examine the effect of noise on threshold error, we add to the histogram a Gaussian white noise, with variance ranging between 0 and 60. The threshold error is given by:

$$Error = \frac{|T(real) - T(estimated)|}{T(real)}$$

The threshold error is presented in Figure 5 as a function of noise variance. According to this figure, we can deduce that the influence of noise on threshold estimation is low.

4.2 Real Histogram

In this section, the thresholding method is applied to three RADARSAT SAR images which are given in Table 2. For each real SAR image, we applied a median filter three times, with mask size (3x3). We then constructed its histogram and applied the thresholding method to this histogram. Finally, we applied the thresholds to the filtered image to obtain a segmented image. The results for SAR images whose dimensions 512x512, 1000x1000 and 532x600 are presented in Figures 6, 7 and 8 respectively. According to Table 2 and the results presented in Figures 6(d), 7(d), and 8(d), we conclude that the influence of the initial parameters on the estimated statistics is low. In Figure 7, the histogram has two modes which are not well separated. We note that the maximum-likelihood technique is able to estimate the statistics. In Figure 8, the statistics for the third mode are not accurate. This is a special case.

5 Conclusion

A thresholding method for SAR segmentation has been proposed. Its principal characteristics are: a) Unlike the methods usually proposed which are limited to bimodal histograms [10]. The method proposed here involoves a multi-modal thresholding; b) the Gamma maximum likelihood technique is used to estimate histogram parameters; c) thresholds are selected by minimizing the error in discrimination between the classes in the image; d) the addition of Gaussian white noise to the histogram has little effect on threshold estimation; and e) the influence of initial parameters on estimated parameters is low. We have tested this algorithm on

Dimensions	512x512	1000x1000	532x600
N	8	4	8
M	2	2	3
$\mu^0(1)$	5	20	90
$\mu^0(2)$	80	50	100
$\mu^0(3)$			230
$P^0(1)$	0.8	0.8	0.6
$P^0(2)$	0.2	0.2	0.1
$P^0(3)$			0.3

Table 2: Input to the thresholding algorithm: Real RADARSAT SAR image, number of looks, number of modes, and initial parameters of the histogram.

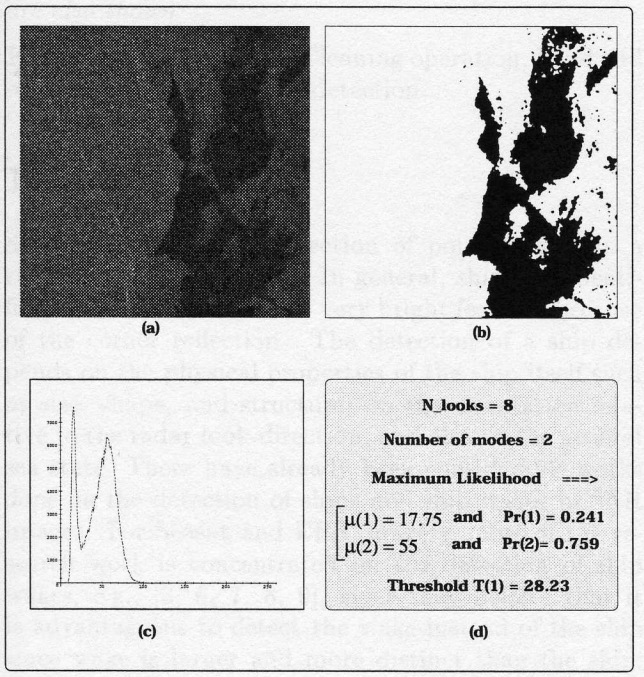

Figure 6: (a) Original RADARSAT SAR image (512x512),(b) Segmented image, (c) Histogram of filtered image and (d) Estimated parameters and threshold.

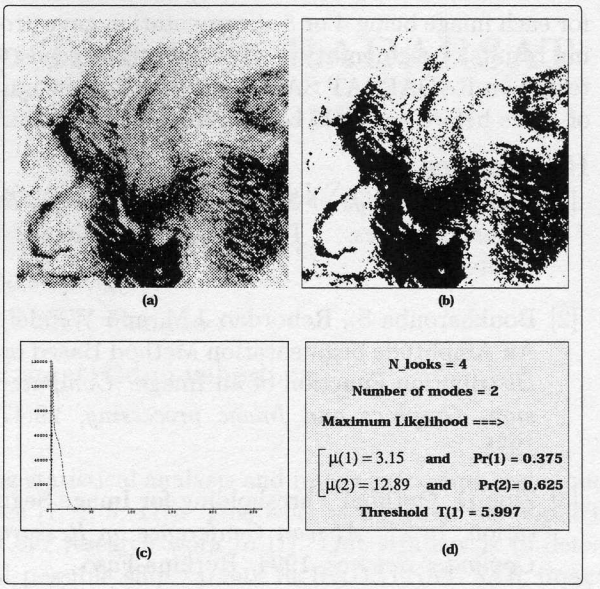

Figure 7: (a) Original RADARSAT SAR image (1000x1000), (b) Segmented image, (c) Histogram of filtered image and (d) Estimated parameters and threshold.

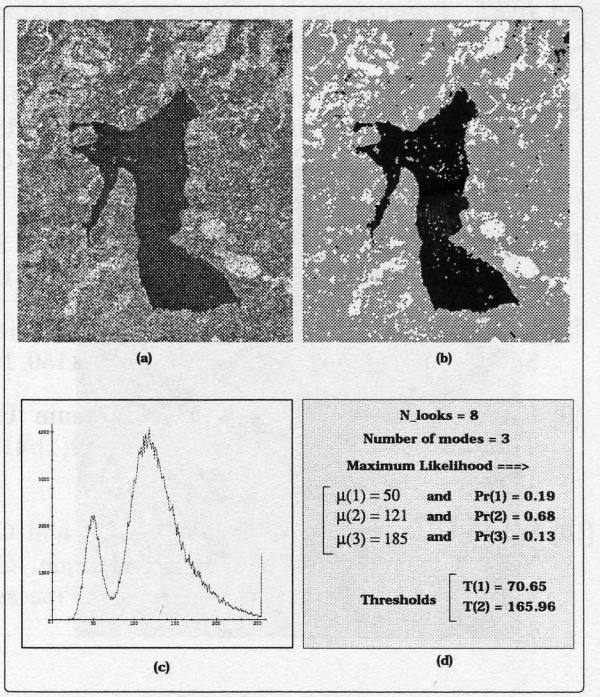

Figure 8: (a) Original RADARSAT SAR image (532x600), (b) Segmented image, (c) Histogram of filtered image and (d) Estimated parameters and thresholds.

several RADARSAT SAR images, the number of looks for each image being 4 or 8. Segmentation gave promising results of segmentation. The algorithm needs to be tested on RADARSAT SAR images with a low number of looks before any final conclusions can be drawn.

References

[1] Saad A. *Filtrage et Segmentation d'Images Radar Polarimétriques.* Ph.D. thesis, Université de Nantes, 1996.

[2] Boukharouba S., Rebordao J.M. and Wendel P.L. An Amplitude Segmentation Method Based on the Distribution Function of an Image. *Computer Vision, Graphics and Image processing*, 29:47–59, 1985.

[3] Ziou D. Optimal Thresholding for Image Segmentation. In 2^{nd} *African Conference on Research in Computer Science*, 1994. Burkina-Faso.

[4] El Zaart A., Ziou D., Bénié G.B., Wang S. and Jiang Q. Oil Spills Detection in SAR Imagery. Technical Report 211, Département de mathématiques et d'Informatique, January 1998.

[5] Ulaby F.T., Kouyate F., Brisco B., and Williams T.H.L. Textural Information in SAR Images. *IEEE Transactions on Geoscience and Remote Sensing*, GE-24(2):235–245, March 1986.

[6] Jiang Q., Wang S., Ziou D., El Zaart A., Bénié G.B., and Rey M. Ship Detection in RADARSAT SAR Imagery. In *Proceedings of IEEE SMC'98*, 1998. (San Diego).

[7] Lee J.S. Speckle Suppression and Analysis for SAR Images. *Optical Engineering*, 25(5):636–643, 1986.

[8] Goodman J.W. Some Fundamental Properties of Speckle. *J. Opt. Soc. Am.*, 66(11):1145–1150, 1976.

[9] Kittler J. and Illingworth J. Minimum Error Thresholding. *Pattern Recognition*, 19(1):41–47, 1986.

[10] Sahoo P.K., Soltani S., Wong A.K.C., and Chen Y.C. A Survey of Thresholding Technique. *Computer Vision, Graphics and Image Processing*, 41:233–260, 1988.